Published in final edited form as:
Acta Biomater. 2015 March ; 14: 43–52. doi:10.1016/j.actbio.2014.12.007.

PEG-diacrylate/hyaluronic acid semi-interpenetrating network compositions for 3D cell spreading and migration

Ho-Joon Lee, **Atanu Sen**, **Sooneon Bae**, **Jeoung Soo Lee**, and **Ken Webb***
Microenvironmental Engineering Laboratory, Department of Bioengineering, Clemson University, 301 Rhodes Research Center, Clemson, SC 29634, USA

Abstract

To serve as artificial matrices for therapeutic cell transplantation, synthetic hydrogels must incorporate mechanisms enabling localized, cell-mediated degradation that allows cell spreading and migration. Previously, we have shown that hybrid semi-interpenetrating polymer networks (semi-IPNs) composed of hydrolytically degradable PEG-diacrylates (PEGdA), acrylate-PEG-GRGDS, and native hyaluronic acid (HA) support increased cell spreading relative to fully synthetic networks that is dependent on cellular hyaluronidase activity. This study systematically investigated the effects of PEGdA/HA semi-IPN network composition on 3D spreading of encapsulated fibroblasts, the underlying changes in gel structure responsible for this activity, and the ability of optimized gel formulations to support long-term cell survival and migration. Fibroblast spreading exhibited a biphasic response to HA concentration, required a minimum HA molecular weight, decreased with increasing PEGdA concentration, and was independent of hydrolytic degradation at early time points. Increased gel turbidity was observed in semi-IPNs, but not in copolymerized hydrogels containing methacrylated HA that did not support cell spreading; suggesting an underlying mechanism of polymerization-induced phase separation resulting in HA-enriched defects within the network structure. PEGdA/HA semi-IPNs were also able to support cell spreading at relatively high levels of mechanical properties (~10 kPa elastic modulus) compared to alternative hybrid hydrogels. In order to support long-term cellular remodeling, the degradation rate of the PEGdA component was optimized by preparing blends of three different PEGdA macromers with varying susceptibility to hydrolytic degradation. Optimized semi-IPN formulations supported long-term survival of encapsulated fibroblasts and sustained migration in a gel-within-gel encapsulation model. These results demonstrate that PEGdA/HA semi-IPNs provide dynamic microenvironments that can support 3D cell survival, spreading, and migration for a variety of cell therapy applications.

*Corresponding author: (864)-656-7603, kwebb@clemson.edu.

Keywords

hybrid hydrogel; semi-interpentrating polymer network; PEG-diacrylate; hyaluronic acid; cell spreading

1. Introduction

Hydrogels have been widely investigated as matrices for therapeutic cell transplantation based upon their ability to be delivered using minimally invasive methods, crosslinked in situ under mild conditions, and provide viscoelastic mechanical properties similar to many soft tissues [1,2]. Conventionally, hydrogels for tissue engineering applications have been prepared from either naturally-derived or synthetic macromolecules. Many naturally-derived materials such as collagen, fibrin, and hyaluronic acid (HA) form hydrogels that intrinsically support cell adhesion and cell-mediated enzymatic degradation. However, these networks possess relatively limited mechanical properties and can be vulnerable to rapid degradation and contraction unless stabilized with additional crosslinking agents. Hydrogels formed from synthetic materials such as polyethylene glycol (PEG) offer superior control over the network physical and chemical properties, but lack intrinsic bioactivity to support cell adhesion and cell-mediated degradation. Many recent efforts in the field have sought to create hybrid or biosynthetic hydrogels composed of both naturally-derived and synthetic materials that combine the strengths and minimize the limitations of each type of material when used alone [3–5].

One of the most prominent strategies for the creation of hybrid hydrogels has been the modification of synthetic networks with oligopeptides derived from natural extracellular matrix (ECM) molecules, including the RGD sequence to support cell adhesion and matrix metalloproteinase (MMP)-substrate sequences to support proteolytic degradation [6,7]. Recent work in this field has shown that hybrid networks containing RGD and MMP-sensitive peptides are effective 3D matrices for the culture of a variety of cell types and support cell proliferation, migration, and ECM deposition [8–10]. When combined with growth factors, various types of PEG-peptide hydrogels have been shown to support bone regeneration and angiogenesis *in vivo* [9,11–15]. Despite their success, there are several limitations to peptide-based hybrid hydrogels. First, oligopeptides are difficult to synthesize in large quantities and expensive while most tissue defects requiring cell-based therapy are relatively large [16]. In addition, most oligopeptides are linear sequences of amino acids only possessing primary structure, resulting in reduced degradation kinetics relative to the native macromolecules from which they are derived [17]. Consequently, gel formulations that support cellular activity are frequently prepared at low polymer concentrations and crosslinking densities, severely limiting their mechanical properties [9,18–20]. This has led several groups to explore screening alternative peptide sequences and strategies for increasing the number of degradable sites [10,21–23].

Alternatively, the use of intact or modified naturally-derived macromolecules to form hybrid hydrogels offers several benefits including substantially lower cost and preservation of native structure potentially supporting higher rates of enzymatic degradation and greater diversity of bioactivity [24]. For example, PEGylated fibrinogen derivatives have been used

to prepare hybrid hydrogels with improved control over mechanical properties and degradation rate compared to native fibrin that have been used for orthopaedic, neural, and cardiovascular applications [25–29]. Hybrid hydrogels based on chemically-modified HA crosslinked with reactive PEG derivatives have been investigated as degradable adhesion barriers and vocal fold augmentation materials [30–32]. While the above studies have used co-polymer networks, our group has recently investigated the possibilities of semi-interpenetrating polymer networks (semi-IPNs) composed of hydrolytically degradable PEG-diacrylates (PEGdA) and native HA [33–35]. We have previously shown that these hydrogels support increased cell spreading and proliferation relative to fully synthetic networks that is dependent on cellular hyaluronidase activity. The objective of the present study was to systematically examine the effects of PEGdA/HA semi-IPN network composition on cell spreading. 3D spreading of encapsulated fibroblasts exhibited a biphasic response to HA concentration, required a minimum HA molecular weight, decreased with increasing PEGdA concentration, and was independent of hydrolytic degradation at early time points. Incorporation of native HA increased gel turbidity, suggesting a potential mechanism of microphase separation resulting in HA-enriched defects in the network structure. Finally, semi-IPNs with optimized PEGdA degradation rate and HA formulation supported sustained 3D cell migration in a gel-within-gel encapsulation model.

2. Materials and Methods

2.1. Synthesis of PEGdA macromers with ester linkages containing variable alkyl spacers

Three different types of PEGdA macromers with varying susceptibility to hydrolytic degradation were synthesized by a two-step process as previously reported [35]. Briefly, PEG (4000 MW, Fluka, Buchs, Switzerland) was reacted with either chloroacetyl chloride, 2-chloropropionyl chloride, or 4-chlorobutuyrl chloride (Sigma-Aldrich, St. Louis, MO) in the presence of triethylamine (TEA, Sigma) at a 1:4:1.8 molar ratio in dry dichloromethane (Sigma). After 24 hours reaction at room temperature, the reactants were filtered, washed with sodium bicarbonate and water, dried with anhydrous sodium sulfate, and then precipitated in ethyl ether. After recovery, each resulting intermediate product was reacted with sodium acrylate (5X molar ratio) in dry dimethylformamide (Acros, Morris Plains, NJ) for 30 hours at 50, 85, and 100 °C to yield PEG-bis-(acryloyloxy acetate) [PEG-bis-AA], PEG-bis-(acryloyloxy propanoate) [PEG-bis-AP], and PEG-bis-(acryloyloxy butyrate) [PEG-bis-AB], respectively. The products were purified by filtration, rotary evaporation, and precipitation in ethyl ether and dried under vacuum. The structures of each PEGdA and the degree of acrylation were determined from the ^{1}H-NMR (Brucker 300 MHz, $CDCl_3$) spectra. All samples achieved acrylation efficiencies greater than 90%.

2.2. Synthesis of methacrylated HA (GMHA)

GMHA was synthesized as previously described [34]. Briefly, HA (1g, MW:1.5 MDa, LifeCore Biomedical, Chaska, MN) was dissolved at 1% (w/v) concentration in deionized water and then TEA (7.33 mL), glycidyl methacrylate (7.33 ml, Acros), and tetrabutyl ammonium bromide (7.33 g, Acros) were added with 3 hours mixing between addition of each reagent. The reaction was allowed to proceed for 12 hours at room temperature

followed by 1 hour at 60 °C. The GMHA product was precipitated in acetone, re-dissolved in deionized water, dialyzed, and recovered by lyophilization.

2.3. Cell culture

Adult normal human dermal fibroblasts (NHDF, Lonza, Walkersville, MD) were cultured in 75 cm^2 tissue culture flasks with DMEM/F-12 50:50 1X media (Mediateach, Herdon, VA) with L-glutamine supplemented with 10% (v/v) bovine growth serum (Hyclone, Logan UT), and 50 U/mL penicillin and 50 μg/mL streptomycin (Mediatech). Medium was changed every 2 days and cells were passaged at a 1:3 ratio for expansion. All encapsulation studies were done with cells between passages 4 and 5.

2.4. Effect of semi-IPN network composition on fibroblast morphology

HA and GMHA (1.75% w/v) and PEGdA (30% w/v) stock solutions were prepared in 1X-PBS (0.1 M, pH 7.4). Acryl-PEG-GRGDS was synthesized by conjugating GRGDS peptide (Bachem, Torrance, CA) to acryl-PEG-NHS (Jenkem, Beijing, China) as previously described [7]. Based upon pilot studies, 6% w/v PEG-bis-AP containing 0.36% w/v 1.5 MDa HA was selected as an initial baseline gel composition. In order to systematically investigate the effect of semi-IPN network composition on the morphology of encapsulated fibroblasts, a series of studies was performed in which one parameter of the gel composition (HA concentration, HA molecular weight, PEGdA concentration, PEGdA chemistry) was varied while the others were held constant (Table I). 250 μl gel precursor solutions were prepared containing PEGdA and HA at varying concentrations, acryl-PEG-GRGDS (1 μmol/mL), 2-hydroxy-1-[4-(hydroxyethoxy) phenyl]-2-methyl-1-propanone (I-2959, BASF, Florham Park, NJ, 0.1% w/v), and NHDF (5×10^6 cells/mL). Sample volumes (50 μl) were pipetted in between glass coverslips separated by 1 mm Teflon spacers and exposed to low intensity UV light (365nm, 10mW/cm^2, Blak-Ray B100-AP, Upland, CA) for 5 minutes on each side of the disc as previously described [34]. Hydrogels with encapsulated cells were cultured in Petri dishes (BD, San Jose, CA) with 3mL culture medium. For studies examining the effect of HA concentration, homogeneous synthetic PEGdA hydrogels (no HA) and co-polymer networks in which native HA was replaced with the same concentrations of GMHA were also prepared. For the study examining the effect of PEGdA concentration, the HA concentration was also varied in order to maintain the 6% w/w ratio of HA:PEGdA present in the baseline gel composition with 6% w/v PEGdA and 0.36% w/v HA. Gels containing encapsulated cells (n=4 samples/group) were cultured for 7 days, fixed with 4% paraformaldehyde (Sigma-Aldrich) in 1X-PBS for 1 hour, permeabilized with 0.1% Triton X-100 (Sigma-Aldrich) in 1X-PBS for 5 minutes and, stained with Alexa Fluor 647-phalloidin (Life Technologies, Grand Island, NY). Samples were imaged using Nikon Ti-Eclipse confocal microscope. Cell morphology at 200μm depth inside hydrogel was visualized and compared to assess cell spreading and network connectivity. Cell circularity (dimensionless parameter defined as circularity = $4\pi/(\text{area}/\text{perimeter}^2)$, ranging from 0 to 1, with 1 being a perfect circle) was calculated from confocal images using the NIH Image J Software Analyze Particles feature.

2.5. Hydrogel turbidity and mechanical properties

To assess gel turbidity, PEG-bis-AP semi-IPNs (6% w/v, 100 μL volume) with varying HA concentration/molecular weight and copolymerized hydrogels with GMHA without NHDF cells (n=4 per group) were photopolymerized as described above. As an additional control, semi-IPNs were also prepared with 0.36% w/v dextran (80 and 1100 kDa, Sigma). The sample discs were placed in 24 well plates and absorbance was measured at 570 nm using μQuant UV-VIS spectrophotometry (BIO-TEK Instruments). The final absorbance values were normalized by subtracting the average value of blank wells. Turbidity was calculated as Turbidity = $-\ln(10^{-A})$, where A=absorbance.

To measure hydrogel mechanical properties, semi-IPNs composed of 1) PEG-bis-AP (6% w/v) with varying concentrations of HA and 2) varying concentrations of PEG-bis-AP with HA maintained at 6% w/w HA:PEGdA were photopolymerized as described above. Hydrogels were cut into dumbbell shaped samples with 30 mm gauge length, 5 mm width, and 1 mm thickness. The samples (n=3/group) were subjected to 35% strain at 5 mm/min using an MTS Synergy 100 (MTS Systems Corporation) at room temperature. Each sample was tested three times to ensure that slippage did not occur.

2.7. Hydrogel degradation study

To evaluate the effect of PEGdA macromer chemistry on hydrogel degradation, semi-IPNs were crosslinked as 1) homogeneous networks containing each of the 3 different PEGdAs and 2) blended networks composed of all 3 PEGdAs mixed in varying ratios. All samples were prepared at 6% w/v total PEGdA concentration with 0.36% HA w/v (1.5 MDa). After photopolymerization, samples were equilibrated with NHDF culture medium with 0.1% w/v sodium azide (Sigma-Aldrich), washed with deionized water, lyophilized, and weighed (Wd_0). Samples were incubated in 4mL of cell culture media with sodium azide in scintillation vials in a cell culture incubator with 5% CO_2 supply at 37 °C. Medium was changed once every 2 days. At each time point, samples (n=3/group) were collected, washed with deionized water, lyophilized, and weighed (Wd_t). Percent mass loss was calculated as $[(Wd_0-Wd_t)/Wd_0]\times100$.

2.8. NHDF morphology and migration in PEGdA blend/HA semi-IPNs

PEGdA macromer blend (12.5% PEG-bis-AA; 37.5% PEG-bis-AP; 50.0% PEG-bis-AB) at 6% w/v final concentration was prepared with 0.36% w/v HA (MW: 1.5 MDa) and acrylate-PEG-GRGDS (1 μmol/mL) and I-2959 (0.1%). In order to evaluate fibroblast morphology during long-term culture, NHDF (10×10^6 cells/mL final concentration) were uniformly dispersed within the gel precursor solution and photopolymerized as described above. Hydrogel samples (n=4/time point) were cultured in 35 mm Petri dishes for 3, 7, 14, 21, 28, and 35 days, then fixed and stained with Alexa 647-phalloidin and imaged by confocal microscopy. To assess the gel's capacity to support cellular invasion and migration, a gel-within-gel encapsulation system was used. NHDF were first entrapped within small fibrin clots (120,000 cells/4 μl) prepared from 1% human fibrinogen (Enzyme Research Laboratories) with 2.5 mM calcium chloride (Sigma) and 0.001 U/mL thrombin (Enzyme Research Laboratories). After gelation for 15 minutes at 37°C, NHDF-loaded fibrin clots were gently placed within 50 μl solutions of the semi-IPN formulation described above

(without additional cells) and gels formed by photopolymerization. As controls, NHDF-loaded fibrin clots were also polymerized within hydrogels of the same composition without native HA and co-polymerized networks with comparable concentrations of GMHA. Hydrogel samples were imaged at day 0, 3, 7, 10, 14, 18, and 21 using phase contrast microscopy (Zeiss). For 3D images, NHDF-loaded fibrin clots were harvested at day 14 and prepared for confocal microscopy as described above. Samples were three dimensionally scanned with 20 μm z-interval.

2.9. Statistical analysis

Quantitative data for hydrogel turbidity and elastic modulus were compared by ANOVA using Tukey's method for post-hoc comparisons (one-way ANOVA followed by Bonferroni's multiple comparison test). p values < 0.05 were considered to be statistically significant. All quantitative data are presented as mean ± standard deviation.

3. Results

3.1. Effect of HA concentration on 3-D fibroblast morphology

NHDF were encapsulated in photopolymerized PEG-bis-AP hydrogels, PEG-bis-AP/HA semi-IPNs containing varying concentrations of HA, and PEG-bis-AP/GMHA copolymer hydrogels. After 7 days in culture, cells in PEG-bis-AP hydrogels without HA were unable to spread and retained a spherical morphology (Figure 1A). In contrast, PEG-bis-AP/HA semi-IPNs supported extensive cell spreading that qualitatively appeared to be greatest at 0.36 and 0.54% HA and moderately decrease at 0.72% HA and higher (Figure 1 B–E), although all samples had circularity values ranging between 0.11–0.14 with no significant differences among these groups. Cells within copolymer hydrogels formed with comparable amounts of GMHA were unable to spread (Figure 1F). Circularity values were significantly lower in all semi-IPNs relative to both PEG-bis-AP hydrogels and PEG-bis-AP/GMHA copolymer hydrogels (Figure 1G). Collectively, these results demonstrate that the ability of PEG-bis-AP/HA semi-IPNs to support cell spreading is a unique property of the semi-IPN network structure.

3.2 Physico-chemical characterization of PEG—bis-AP/HA semi-IPNs and hydrogels

The effect of HA incorporation on hydrogel physico-chemical properties was analyzed by measuring turbidity and tensile properties. Figure 2 shows the turbidity of both PEG-bis-AP/HA semi-IPNs and PEG-bis-AP/GMHA copolymer hydrogels measured by spectrophotometry. Relative to PEG-bis-AP hydrogels, incorporation of native HA to form semi-IPNs significantly increased sample turbidity in a dose-dependent manner. The turbidity of copolymer hydrogels containing comparable amounts of GMHA was not significantly different than the PEG-bis-AP control at any concentration tested.

The mechanical properties of PEG-bis-AP/HA semi-IPNs were measured by tensile testing. The elastic modulus of semi-IPNs containing 0.18% w/v HA was modestly higher than the PEG-bis-AP hydrogel without HA and then elastic moduli values decreased with increasing HA content with the differences being statically significant at the two highest concentrations (Figure 3).

3.3. Effect of HA molecular weight on 3-D fibroblast morphology and gel turbidity

NHDF were encapsulated in semi-IPNs containing 6% w/v PEG-bis-AP and 0.36% w/v HA of varying molecular weight (MW). Semi-IPNs containing low MW (100 kDa) HA did not support the spreading of fibroblasts, which retained a spherical morphology after 7 days in culture (Figure 4). At 700 kDa HA MW and higher, all samples exhibited comparable cell spreading and significantly lower circularity values than semi-IPNs prepared with 100 kDa HA. These results demonstrate that a minimum threshold for HA MW exists that is required to support cell spreading. The turbidity of semi-IPNs significantly increased for all HA MWs tested relative to the PEGdA only control, however, the turbidity of semi-IPNs containing 100 kDa HA was significantly lower than all three groups containing higher molecular weight HA (Figure 5). Semi-IPNs prepared with comparable amounts of both low (80 kDa) and high (1100 kDa) MW dextran did not exhibit significant changes in turbidity relative to the PEGdA control.

3.4. Effect of PEG diacrylate macromer concentration and chemical structure on 3-D fibroblast morphology

NHDF were encapsulated in semi-IPNs containing various concentrations of PEG-bis-AP and HA, maintaining constant 6% w/w PEG/HA ratio. Semi-IPNs containing 4–6% PEG-bis-AP effectively supported cell spreading at 7 days with the most robust response observed at the 4% concentration (Figure 6). Cell spreading was substantially reduced as the PEG-bis-AP concentration was increased to 8% and minimally present at 10%. Circularity values steadily increased with increasing PEGdA concentration, although the maximum value reached at 10% PEGdA (0.32±0.02) was significantly lower than that observed in PEGdA hydrogel controls without HA (0.65 ± .08, Figure 1). Tensile testing showed that semi-IPN elastic modulus increased from 10.2 +/− 2.07 kPa at 6% to 28.0 w/v +/−2.65 kPa and 76.0 +/− 3.61 kPa at 8 and 10% concentration, respectively. Samples prepared at 4% were visibly weaker and could not be evaluated by tensile testing.

NHDF were also encapsulated in semi-IPNs prepared from various PEGdA macromers with varying chemical structures (PEG-bis-AA, PEG-bis-AP, or PEG-bis-AB) previously shown to provide different susceptibility to hydrolytic degradation [35]. As early as 3 days post-encapsulation, fibroblast spreading was observed in all semi-IPN compositions with no significant differences in circularity values (Figure 7). Cells encapsulated within homopolymer hydrogels of even the most rapidly hydrolytically degrading macromer (PEG-bis-AA) without HA did not exhibit any spreading (data not shown). These results confirm that the initiation of cell spreading within these gels is attributable to the HA component and independent of PEG macromer chemistry and hydrolytic degradation.

3.5. Degradation kinetics of various semi-IPNs

In preparation for longer-term studies, the hydrolytic degradation kinetics of semi-IPNs prepared from PEGdA macromers with varying chemical structure were studied during incubation in serum-containing medium. For semi-IPNs prepared from each of the three different PEGdA macromers individually, PEG-bis-AA semi-IPNs showed the fastest degradation rate (complete degradation at day 7), PEG-bis-AP showed intermediate degradation rate (complete degradation at day 18), and PEG-bis-AB based semi-IPNs

showed the slowest degradation rate (ca. 34% mass loss at day 42) (Figure 8A). In order to achieve a broader range of degradation profiles, blended PEGdA compositions (C1–C7, Figure 8B) containing the 3 different PEGdA macromers in various ratios were evaluated. A gel composition consisting of 12.5 % PEG-bis-AA, 37.5% PEG-bis-AP, and 50% PEG-bis-AB ('C1') was found to exhibit relatively linear mass loss over 5 weeks and was used for all further studies.

3.6. Long-term 3-D fibroblast culture in blended PEGdA/HA semi-IPNs

In the first long-term culture study, NHDF were homogeneously encapsulated within semi-IPNs (6% w/v 'C1' PEGdA blend/0.36% w/v HA) and cultured for 35 days. As shown in Figure 9, NHDF spreading progressively increased over the culture period and the cell number exhibited little change, suggesting limited cell proliferation. This is in contrast to blended PEGdA only (no HA) or blended PEGdA/GMHA hydrogel controls, where cells remained restricted to a spherical morphology and cell number visibly decreased by approximately 50% within 14 days (data not shown).

In order to assess the ability of NHDF to migrate through blended PEGdA/HA semi-IPNs, NHDF were pre-encapsulated within fibrin clots that were subsequently entrapped within semi-IPNs during photopolymerization. Within 3 days, NHDF began to migrate out of the fibrin clots into the surrounding semi-IPNs (Figure 10A). NHDF migration progressively increased over time, reaching 1.5 mm depth within 21 days (Figure 10B–D). NHDF-loaded fibrin clots encapsulated within blended PEGdA/GMHA copolymer hydrogels as a control exhibited limited migration into the surrounding gel after 21 days in culture (Figure 10E). 3D confocal reconstruction confirmed that NHDF-loaded clots and cellular outgrowth was occurring within the 3D network volume rather than on the gel surface (Figure 10F).

4. Discussion

The efficacy of cell-based therapy can be substantially improved by the use of scaffolds that serve as a provisional matrix for cell adhesion, migration, and proliferation. Synthetic hydrogels offer injectable matrices with defined structure and composition; however, such networks generally possess nanometer-scale mesh sizes that restrict encapsulated cells to a spherical morphology. For most anchorage-dependent cell types, the ability to adopt a spread morphology is essential for survival, migration, proliferation, and differentiation [36–38]. Therefore, there is a critical need for the development of hybrid networks incorporating naturally-derived components that support localized, cell-mediated remodeling.

As an alternative to the prevailing approach of crosslinking synthetic macromolecules with protease-sensitive oligopeptides, our group has previously shown that semi-IPNs composed of hydrolytically degradable PEG diacrylates and native HA support rapid 3D cell spreading in a hyaluronidase-dependent manner [33]. These materials are attractive candidates because other PEG and HA derivatives have been successfully translated for clinical applications [39,40]. In this study, we systematically examined the effect of semi-IPN network composition on 3D cell spreading, beginning with a baseline gel formulation composed of 6% w/v PEG-bis-AP macromer that provides an intermediate rate of hydrolytic degradation and 0.36% w/v HA (1.5 MDa). Fibroblast spreading in 3D exhibited a biphasic response to

varying the concentration of HA, initially increasing at levels higher that those originally tested by Kutty et al. (0.18% w/v) [33], then subsequently declining at 0.72% or higher. We hypothesized that the ability of these semi-IPNs to support cell spreading originates from polymerization-induced phase separation as previously suggested by Ouasti et al. [41]. In support of this hypothesis, fibroblast spreading was completely eliminated when native HA was replaced with a methacrylated HA derivative (GMHA) that could be covalently incorporated into the network, thereby limiting its potential to undergo phase separation. Gel turbidity was also evaluated as a quantitative measure of phase separation and found to increase with increasing HA concentration in semi-IPNs, but not copolymerized hydrogels containing GMHA. Finally, when the HA molecular weight was varied, it was observed that cell spreading required relatively high HA molecular weight, consistent with the increased tendency for phase separation as solute molecular weight increases. Interestingly, semi-IPNs prepared with dextran, even at high molecular weight, did not result in increased gel turbidity. This result suggests that HA is unique among various materials tested for the non-crosslinked component of these semi-IPNs, including collagen and gelatin in previous studies [33], in its ability to induce phase separation, at least to a degree sufficient to create microdomains that allow cell spreading. This is likely attributable to the unique properties of HA in terms of water-binding capacity; H-bonding and self-association; and solution rheology [42].

The ability of cells to spread and migrate in 3D has also been found to be dependent on the hydrogel's mechanical properties [10,18,19]. Tensile testing showed that the elastic modulus of semi-IPNs decreased with increasing HA concentration, likely due to the increasing level of phase separation creating defects within the network structure. However, it is particularly important to note that the elastic moduli values for 6% PEG-bis-AP with 0.36% and 0.54% HA that most effectively supported cell spreading ranged between 8–10 kPa. In contrast, most peptide-crosslinked hydrogels that support cell spreading/migration are characterized by elastic shear moduli values generally around and below 1 kPa, approximately an order of magnitude lower [16,23,43,44]. The higher mechanical properties of PEGdA/HA semi-IPNs offer several advantages including increased mechanical stability and resistance to cell-mediated contraction. In addition, recent studies have shown that substrate mechanics influence stem cell differentiation in both 2D and 3D culture systems and the elastic modulus of PEGdA/HA semi-IPNs is in close approximation to values shown to most efficiently promote osteogenic differentiation of human mesenchymal stem cells [45,46].

We also investigated the effect of variation in PEGdA concentration and chemical composition on 3D fibroblast spreading. Higher polymer concentrations resulted in increased mechanical properties and strongly inhibited cell spreading at PEGdA concentrations of 8% w/v and greater, despite corresponding increases in HA concentration to maintain a constant PEGdA:HA w/w ratio. This observation is consistent with many previous reports in the literature, although as noted above, the range of mechanical properties was much higher in PEGdA/HA semi-IPNs [10,18,19,25,47]. At 6% w/v, all three PEGdA chemical compositions supported the initiation of cell spreading within three days. In combination with previous work showing that the most slowly degrading PEG-bis-AB exhibits negligible mass loss at 3 days [34], this result demonstrates that the initiation of cell spreading in these semi-IPNs is independent of hydrolytic degradation and based solely

upon cell-mediated degradation of HA. The ability of cells to begin spreading rapidly is another important advantage of these PEGdA/HA semi-IPNs relative to peptide-crosslinked networks in which a lag period of 7–14 days is often observed between the time of encapsulation and the initiation of cell spreading, particularly when encapsulation is performed with dissociated individual cells [8,21,22,43,47]. Collectively, these results suggest that photopolyermization-induced phase separation creates HA-enriched defects within the network structure that facilitate rapid hyaluronidase-mediated localized degradation that supports cell spreading.

One challenge to the application of these semi-IPNs for long-term culture and translational applications was that none of the PEGdA macromers when used alone provided an ideal degradation profile. PEG-bis-AA and PEG-bis-AP degraded too rapidly resulting in loss of mechanical integrity and contraction, while PEG-bis-AB degraded too slowly, with little further cell spreading observed beyond that at 3–7 days and subsequent reduction in cellularity at later time points, presumably as a result of cell death. Previously, Quick et al. showed that blending acrylated PLA-b-PEG-b-PLA macromers with different PLA block lengths and therefore hydrolytic degradation rate could produce gels with more finely controlled and linear rates of degradation [48]. We adapted this approach by creating blends of the three different PEGdAs used in this study to obtain a formulation displaying relative linear mass loss over 5 weeks. These degradation studies were performed in serum-containing medium to reflect culture conditions because gel degradation was originally noticed to be much more rapid than previously observed during degradation in PBS, likely due to the contribution of serum esterase enzymes. Using the selected blend formulation of PEGdA, sustained cell spreading and viability was observed for up to 35 days. Finally, a gel-within-gel encapsulation model was used to test the ability of blended PEGdA/HA semi-IPNs to support cell invasion and sustained migration. Fibroblasts pre-encapsulated within fibrin clots began sprouting into the surrounding semi-IPN and progressively migrated radially outward for over 21 days. As in our dispersed cell encapsulation model, copolymer hydrogels prepared with GMHA were unable to support this behavior. These results suggest that the HA-enriched zones created by phase separation are sufficiently inter-connected, in combination with gradual hydrolytic degradation, to support sustained cell migration.

5. Conclusions

These studies demonstrate that through systematic optimization of network composition, PEGdA/HA semi-IPNs can be formulated to provide dynamic microenvironments that support cell survival, spreading, and sustained migration. The bioactivity of these networks is a unique feature of the semi-IPN structure derived from polymerization-induced phase separation that creates HA-enriched micro-domains susceptible to cell-mediated enzymatic degradation in combination with prolonged hydrolytic degradation. Specific advantages of these semi-IPNs relative to existing hybrid hydrogels are the ability to support the rapid initiation of cell spreading within three days post-encapsulation and the provision of improved mechanical properties. Ongoing studies are examining covalent conjugation of bioactive molecules to the HA component of these networks for sequestration and cell-mediated release during network remodeling and applications in orthopaedic tissue engineering.

Acknowledgments

Funding for this project was provided by grant #8P20GM103444 from the National Institute of General Medical Sciences through the SC Bioengineering Center of Regeneration and Formation of Tissues (SC BioCRAFT). The authors gratefully acknowledge Dr. Guzeliya Korneva in the Materials Synthesis, Characterization, and Testing Core for assistance with hydrogel tensile testing and Dr. Terri Bruce and Ms. Rhonda Rogers Powell in the Histology and Imaging Core for assistance with confocal microscopy.

References

1. Nicodemus GD, Bryant SJ. Cell encapsulation in biodegradable hydrogels for tissue engineering applications. Tissue Eng Part B Rev. 2008; 14:149–65.10.1089/ten.teb.2007.0332 [PubMed: 18498217]
2. Slaughter BV, Khurshid SS, Fisher OZ, Khademhosseini A, Peppas Na. Hydrogels in regenerative medicine. Adv Mater. 2009; 21:3307–29.10.1002/adma.200802106 [PubMed: 20882499]
3. Kopecek J. Hydrogel biomaterials: a smart future? Biomaterials. 2007; 28:5185–92.10.1016/j.biomaterials.2007.07.044 [PubMed: 17697712]
4. Jia X, Kiick KL. Hybrid multicomponent hydrogels for tissue engineering. Macromol Biosci. 2009; 9:140–56.10.1002/mabi.200800284 [PubMed: 19107720]
5. Tibbitt MW, Anseth KS. Hydrogels as extracellular matrix mimics for 3D cell culture. Biotechnol Bioeng. 2009; 103:655–63.10.1002/bit.22361 [PubMed: 19472329]
6. West J, Hubbell J. Polymeric biomaterials with degradation sites for proteases involved in cell migration. Macromolecules. 1999:241–4.
7. Hern DL, Hubbell Ja. Incorporation of adhesion peptides into nonadhesive hydrogels useful for tissue resurfacing. J Biomed Mater Res. 1998; 39:266–76. [PubMed: 9457557]
8. Anderson SB, Lin C-C, Kuntzler DV, Anseth KS. The performance of human mesenchymal stem cells encapsulated in cell-degradable polymer-peptide hydrogels. Biomaterials. 2011; 32:3564–74.10.1016/j.biomaterials.2011.01.064 [PubMed: 21334063]
9. Lutolf MP, Raeber GP, Zisch aH, Tirelli N, Hubbell Ja. Cell-Responsive Synthetic Hydrogels. Adv Mater. 2003; 15:888–92.10.1002/adma.200304621
10. Sokic S, Papavasiliou G. Controlled Proteolytic Cleavage Site Presentation in Biomimetic PEGDA Hydrogels Enhances Neovascularization In Vitro. Tissue Eng Part A. 2012; 18:2477–86.10.1089/ten.tea.2012.0173 [PubMed: 22725267]
11. Lutolf MP, Weber FE, Schmoekel HG, Schense JC, Kohler T, Müller R, et al. Repair of bone defects using synthetic mimetics of collagenous extracellular matrices. Nat Biotechnol. 2003; 21:513–8.10.1038/nbt818 [PubMed: 12704396]
12. Ehrbar M, Rizzi SC, Hlushchuk R, Djonov V, Zisch AH, Hubbell Ja, et al. Enzymatic formation of modular cell-instructive fibrin analogs for tissue engineering. Biomaterials. 2007; 28:3856–66.10.1016/j.biomaterials.2007.03.027 [PubMed: 17568666]
13. Mariner PD, Wudel JM, Miller DE, Genova EE, Streubel S-O, Anseth KS. Synthetic hydrogel scaffold is an effective vehicle for delivery of INFUSE (rhBMP2) to critical-sized calvaria bone defects in rats. J Orthop Res. 2013; 31:401–6.10.1002/jor.22243 [PubMed: 23070779]
14. Phelps EA, Landázuri N, Thulé PM, Taylor WR, García AJ. Bioartificial matrices for therapeutic vascularization. Proc Natl Acad Sci U S A. 2010; 107:3323–8.10.1073/pnas.0905447107 [PubMed: 20080569]
15. Leslie-Barbick JE, Saik JE, Gould DJ, Dickinson ME, West JL. The promotion of microvasculature formation in poly(ethylene glycol) diacrylate hydrogels by an immobilized VEGF-mimetic peptide. Biomaterials. 2011; 32:5782–9.10.1016/j.biomaterials.2011.04.060 [PubMed: 21612821]
16. Jo YS, Rizzi SC, Ehrbar M, Weber FE, Hubbell Ja, Lutolf MP. Biomimetic PEG hydrogels crosslinked with minimal plasmin-sensitive tri-amino acid peptides. J Biomed Mater Res A. 2010; 93:870–7.10.1002/jbm.a.32580 [PubMed: 19701911]

17. Chung EH, Gilbert M, Virdi AS, Sena K, Sumner DR, Healy KE. Biomimetic artificial ECMs stimulate bone regeneration. J Biomed Mater Res A. 2006; 79:815–26.10.1002/jbm.a.30809 [PubMed: 16886222]
18. Ehrbar M, Sala a, Lienemann P, Ranga a, Mosiewicz K, Bittermann a, et al. Elucidating the role of matrix stiffness in 3D cell migration and remodeling. Biophys J. 2011; 100:284–93.10.1016/j.bpj.2010.11.082 [PubMed: 21244824]
19. Bott K, Upton Z, Schrobback K, Ehrbar M, Hubbell JA, Lutolf MP, et al. The effect of matrix characteristics on fibroblast proliferation in 3D gels. Biomaterials. 2010; 31:8454–64.10.1016/j.biomaterials.2010.07.046 [PubMed: 20684983]
20. Loessner D, Stok KS, Lutolf MP, Hutmacher DW, Clements Ja, Rizzi SC. Bioengineered 3D platform to explore cell-ECM interactions and drug resistance of epithelial ovarian cancer cells. Biomaterials. 2010; 31:8494–506.10.1016/j.biomaterials.2010.07.064 [PubMed: 20709389]
21. Patterson J, Hubbell Ja. Enhanced proteolytic degradation of molecularly engineered PEG hydrogels in response to MMP-1 and MMP-2. Biomaterials. 2010; 31:7836–45.10.1016/j.biomaterials.2010.06.061 [PubMed: 20667588]
22. Patterson J, Hubbell Ja. SPARC-derived protease substrates to enhance the plasmin sensitivity of molecularly engineered PEG hydrogels. Biomaterials. 2011; 32:1301–10.10.1016/j.biomaterials.2010.10.016 [PubMed: 21040970]
23. Sokic S, Papavasiliou G. FGF-1 and proteolytically mediated cleavage site presentation influence three-dimensional fibroblast invasion in biomimetic PEGDA hydrogels. Acta Biomater. 2012; 8:2213–22.10.1016/j.actbio.2012.03.017 [PubMed: 22426138]
24. Ghosh K, Ren X, Shu X. Fibronectin functional domains coupled to hyaluronan stimulate adult human dermal fibroblast responses critical for wound healing. Tissue Eng Part A. 2006; 12:601–13.
25. Almany L, Seliktar D. Biosynthetic hydrogel scaffolds made from fibrinogen and polyethylene glycol for 3D cell cultures. Biomaterials. 2005; 26:2467–77.10.1016/j.biomaterials.2004.06.047 [PubMed: 15585249]
26. Peled E, Boss J, Bejar J, Zinman C, Seliktar D. A novel poly(ethylene glycol)-fibrinogen hydrogel for tibial segmental defect repair in a rat model. J Biomed Mater Res A. 2007; 80:874–84.10.1002/jbm.a.30928 [PubMed: 17072852]
27. Sarig-Nadir O, Seliktar D. Compositional alterations of fibrin-based materials for regulating in vitro neural outgrowth. Tissue Eng Part A. 2008; 14:401–11.10.1089/tea.2007.0029 [PubMed: 18333792]
28. Zhang G, Drinnan CT, Geuss LR, Suggs LJ. Vascular differentiation of bone marrow stem cells is directed by a tunable three-dimensional matrix. Acta Biomater. 2010; 6:3395–403.10.1016/j.actbio.2010.03.019 [PubMed: 20302976]
29. Zhang G, Wang X, Wang Z, Zhang J, Suggs L. A PEGylated fibrin patch for mesenchymal stem cell delivery. Tissue Eng. 2006; 12:9–19.10.1089/ten.2006.12.9 [PubMed: 16499438]
30. Connors RC, Muir JJ, Liu Y, Reiss GR, Kouretas PC, Whitten MG, et al. Postoperative pericardial adhesion prevention using Carbylan-SX in a rabbit model. J Surg Res. 2007; 140:237–42.10.1016/j.jss.2007.03.014 [PubMed: 17509269]
31. Zheng Shu X, Liu Y, Palumbo FS, Luo Y, Prestwich GD. In situ crosslinkable hyaluronan hydrogels for tissue engineering. Biomaterials. 2004; 25:1339–48.10.1016/j.biomaterials.2003.08.014 [PubMed: 14643608]
32. Hansen JK, Thibeault SL, Walsh JF, Shu XZ, Prestwich GD. In vivo engineering of the vocal fold extracellular matrix with injectable hyaluronic acid hydrogels: early effects on tissue repair and biomechanics in a rabbit model. Ann Otol Rhinol Laryngol. 2005; 114:662–70. [PubMed: 16240927]
33. Kutty JK, Cho E, Soo Lee J, Vyavahare NR, Webb K. The effect of hyaluronic acid incorporation on fibroblast spreading and proliferation within PEG-diacrylate based semi-interpenetrating networks. Biomaterials. 2007; 28:4928–38.10.1016/j.biomaterials.2007.08.007 [PubMed: 17720239]
34. Kutty JK, Webb K. Mechanomimetic hydrogels for vocal fold lamina propria regeneration. J Biomater Sci Polym Ed. 2009; 20:737–56.10.1163/156856209X426763 [PubMed: 19323887]

35. Cho E, Kutty JK, Datar K, Lee JS, Vyavahare NR, Webb K. A novel synthetic route for the preparation of hydrolytically degradable synthetic hydrogels. J Biomed Mater Res A. 2009; 90:1073–82.10.1002/jbm.a.32172 [PubMed: 18671270]
36. Gao L, McBeath R, Chen CS. Stem cell shape regulates a chondrogenic versus myogenic fate through Rac1 and N-cadherin. Stem Cells. 2010; 28:564–72.10.1002/stem.308 [PubMed: 20082286]
37. McBeath R, Pirone DM, Nelson CM, Bhadriraju K, Chen CS. Cell shape, cytoskeletal tension, and RhoA regulate stem cell lineage commitment. Dev Cell. 2004; 6:483–95. [PubMed: 15068789]
38. Chen CS. Geometric Control of Cell Life and Death. Science (80-). 1997; 276:1425–8.10.1126/science.276.5317.1425
39. Kuo, JW. Practical Aspects of Hyaluronan Based Medical Products. CRC Press; 2005.
40. Dick, HB.; Schwenn, O. Viscoelastics in Ophthalmic Surgery. Berlin, Heidelberg: Springer; 2000.
41. Ouasti S, Donno R, Cellesi F, Sherratt MJ, Terenghi G, Tirelli N. Network connectivity, mechanical properties and cell adhesion for hyaluronic acid/PEG hydrogels. Biomaterials. 2011; 32:6456–70.10.1016/j.biomaterials.2011.05.044 [PubMed: 21680016]
42. Cowman MK, Matsuoka S. Experimental approaches to hyaluronan structure. Carbohydr Res. 2005; 340:791–809.10.1016/j.carres.2005.01.022 [PubMed: 15780246]
43. Raeber GP, Lutolf MP, Hubbell Ja. Molecularly engineered PEG hydrogels: a novel model system for proteolytically mediated cell migration. Biophys J. 2005; 89:1374–88.10.1529/biophysj.104.050682 [PubMed: 15923238]
44. Rizzi SC, Ehrbar M, Halstenberg S, Raeber GP, Schmoekel HG, Hagenmüller H, et al. Recombinant protein-co-PEG networks as cell-adhesive and proteolytically degradable hydrogel matrixes. Part II: biofunctional characteristics. Biomacromolecules. 2006; 7:3019–29.10.1021/bm060504a [PubMed: 17096527]
45. Engler AJ, Sen S, Sweeney HL, Discher DE. Matrix elasticity directs stem cell lineage specification. Cell. 2006; 126:677–89.10.1016/j.cell.2006.06.044 [PubMed: 16923388]
46. Huebsch N, Arany PR, Mao AS, Shvartsman D, Ali Oa, Bencherif Sa, et al. Harnessing traction-mediated manipulation of the cell/matrix interface to control stem-cell fate. Nat Mater. 2010; 9:518–26.10.1038/nmat2732 [PubMed: 20418863]
47. Yang PJ, Levenston ME, Temenoff JS. Modulation of mesenchymal stem cell shape in enzyme-sensitive hydrogels is decoupled from upregulation of fibroblast markers under cyclic tension. Tissue Eng Part A. 2012; 18:2365–75.10.1089/ten.TEA.2011.0727 [PubMed: 22703182]
48. Quick DJ, Anseth KS. DNA delivery from photocrosslinked PEG hydrogels: encapsulation efficiency, release profiles, and DNA quality. J Control Release. 2004; 96:341–51.10.1016/j.jconrel.2004.01.021 [PubMed: 15081223]

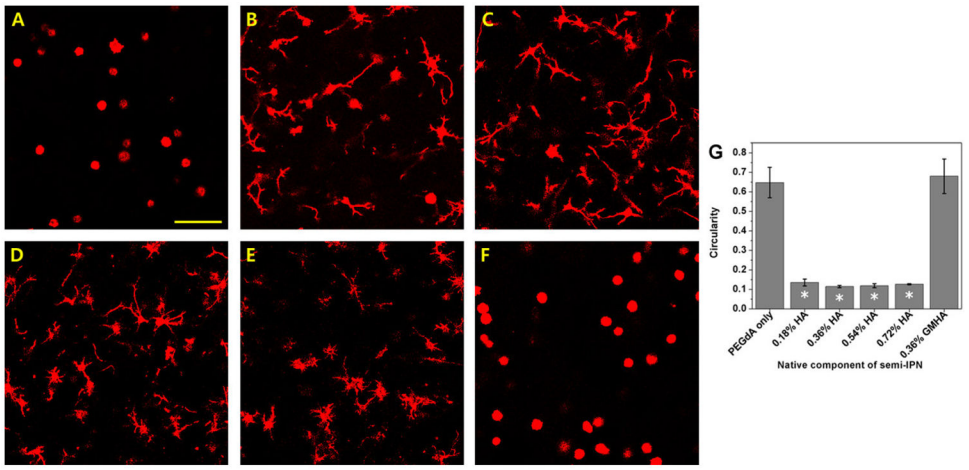

Figure 1.

Confocal microscopy images of actin-stained human dermal fibroblasts encapsulated within 6% w/v PEG-bis-AP hydrogel (A), PEG-bis-AP/HA semi-IPNs containing 0.18% w/v HA (B), 0.36% w/v HA (C), 0.54% w/v HA (D), 0.72% w/v HA (E), and PEG-bis-AP/GMHA co-polymer hydrogel containing 0.36% w/v GMHA (F) at 200 μm depth after 7 days culture and corresponding circularity values (G). Scale bar = 100 μm. *=$p<0.05$ relative to PEG-bis-AP hydrogel.

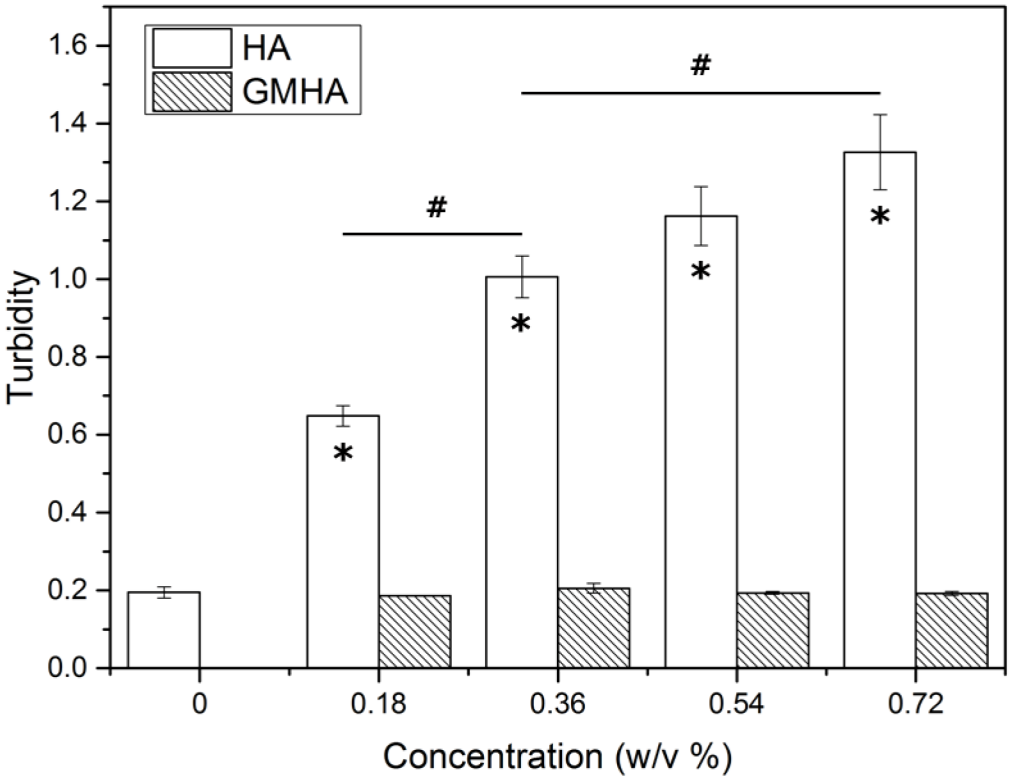

Figure 2.

Turbidity of 6% w/v PEG-bis-AP hydrogels, PEG-bis-AP/HA semi-IPNs containing varying amounts of HA, and PEG-bis-AP/GMHA copolymer hydrogels containing varying amounts of GMHA. *=$p<0.05$ relative to PEG-bis-AP hydrogel and #=$p<0.05$ between groups.

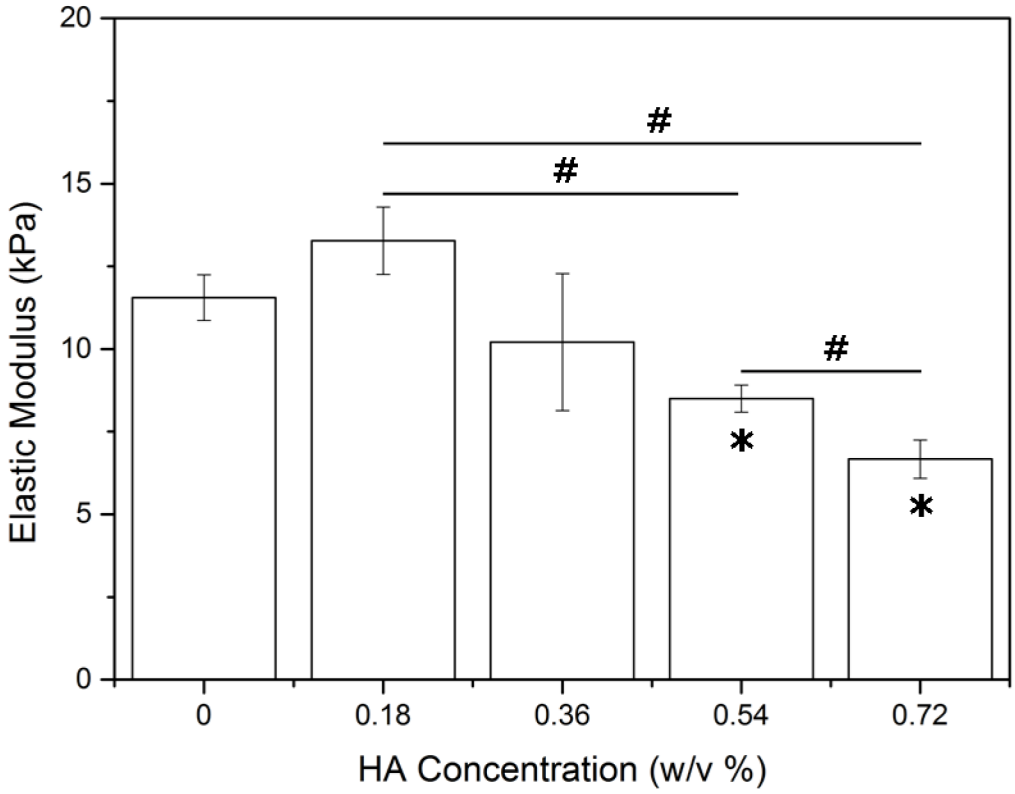

Figure 3.

Elastic modulus of 6% w/v PEG-bis-AP hydrogels and PEG-bis-AP/HA semi-IPNs containing varying amounts of HA. *=$p<0.05$ relative to PEG-bis-AP hydrogel and #=$p<0.05$ between groups.

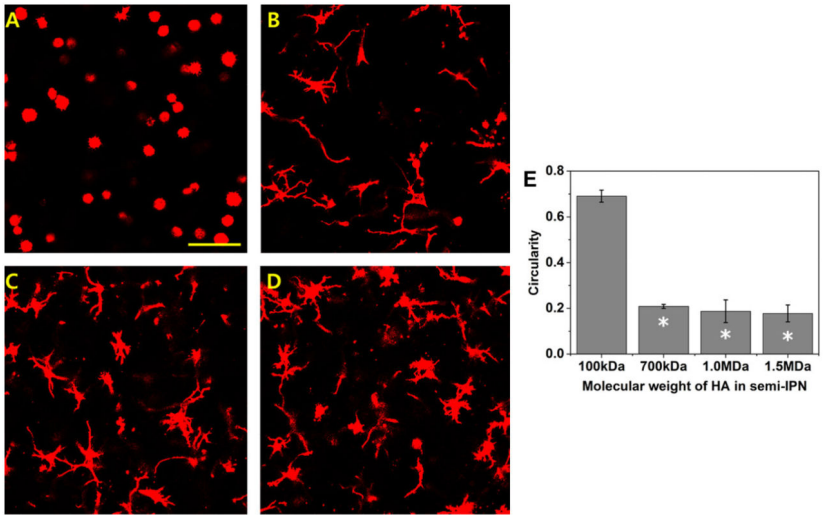

Figure 4.

Confocal microscopy images of actin-stained human dermal fibroblasts encapsulated within 6% w/v PEG-bis-AP/0.36% w/v HA semi-IPNs prepared using HA with molecular weights of 100 kDa (A), 700 kDa (B), 1.0 MDa (C) and 1.5 MDa (D) at 200 μm depth after 7 days culture and corresponding circularity values (E). Scale bar = 100 μm. *=$p<0.05$ relative to PEG-bis-AP/HA semi-IPN with 100 kDa HA.

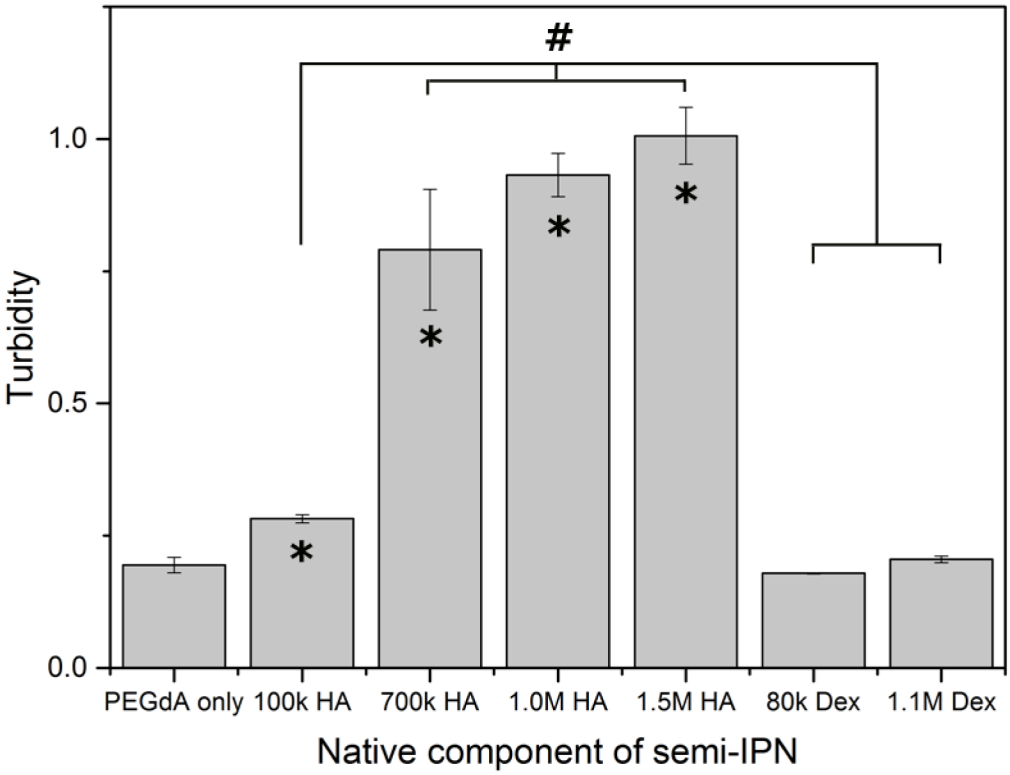

Figure 5.

Turbidity of 6% w/v PEG-bis-AP hydrogel and PEG-bis-AP/HA and PEG-bis-AP/dextran semi-IPNs containing 0.36% w/v HA or dextran of varying molecular weight. *=$p<0.05$ relative to PEG-bis-AP hydrogel and #=$p<0.05$ between groups.

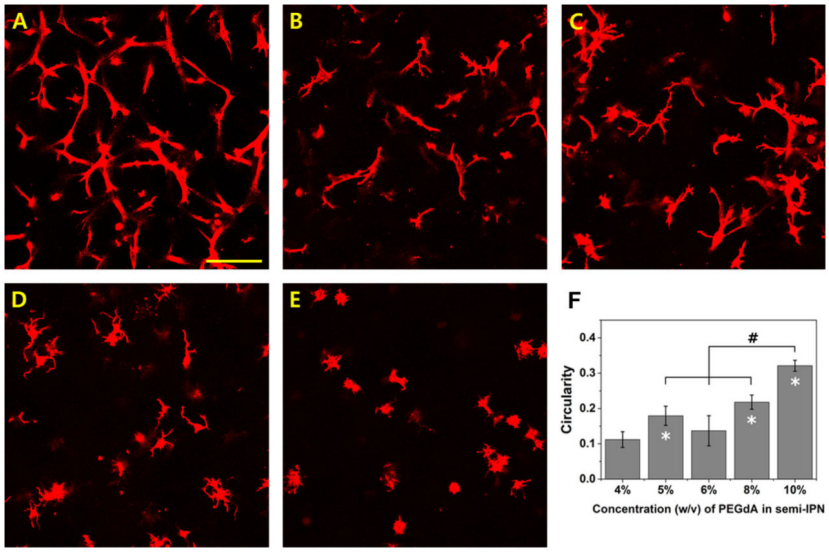

Figure 6.

Confocal microscopy images of actin-stained human dermal fibroblasts encapsulated within PEG-bis-AP/HA semi-IPNs containing varying concentrations of PEG-bis-AP and HA; 4% w/v PEG-bis-AP with 0.24% w/v HA (A), 5% w/v PEG-bis-AP with 0.30% w/v HA (B), 6% w/v PEG-bis-AP with 0.36% w/v HA (C), 8% w/v PEG-bis-AP with 0.48% w/v HA (D) and 10% w/v PEG-bis-AP with 0.60% w/v HA (E) at 200 μm depth after 7 days culture and corresponding circularity values (F). Scale bar = 100 μm. *=$p<0.05$ relative to 4% w/v PEG-bis-AP with 0.24% w/v HA semi-IPN and #=$p<0.05$ between groups.

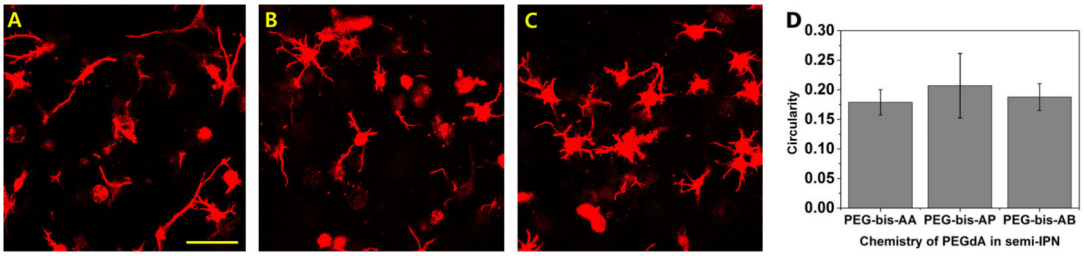

Figure 7.

Confocal microscopy images of actin-stained human dermal fibroblasts encapsulated within 6% w/v PEGdA/0.36% w/v HA semi-IPNs formed from PEG-bis-AA (A), PEG-bis-AP (B), and PEG-bis-AB (C) macromers at 200 μm depth after 3 days culture and corresponding circularity values (D). Scale bar = 100 μm.

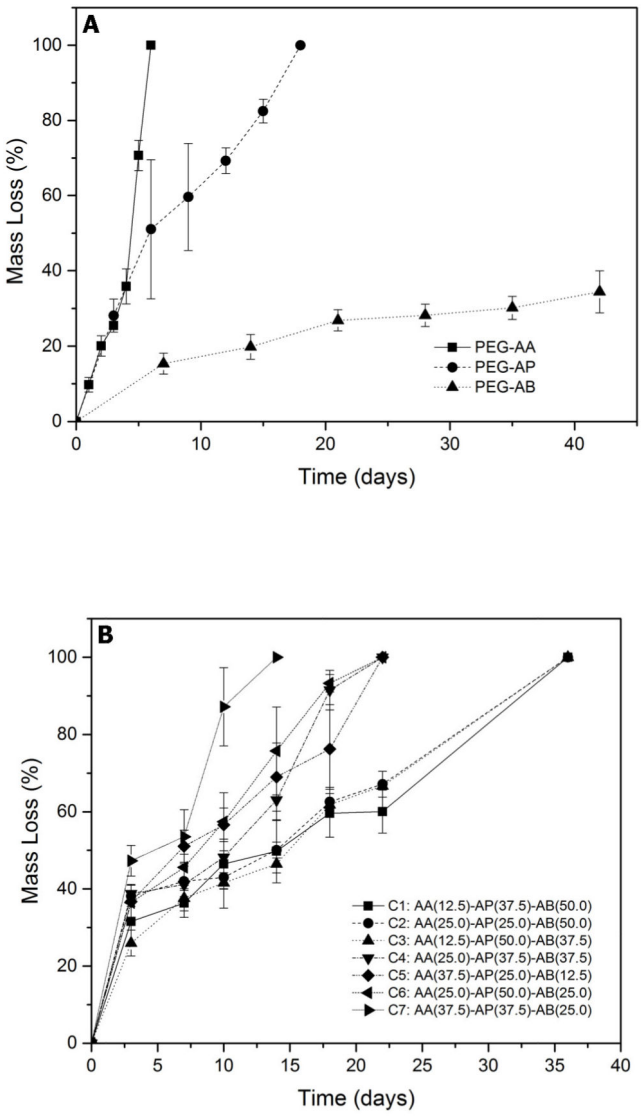

Figure 8.

Mass loss of 6% w/v PEGdA/0.36 % w/v semi-IPNs prepared with homogeneous (A) and blended (B) PEGdA composition in routine culture medium containing 0.1% w/v sodium azide.

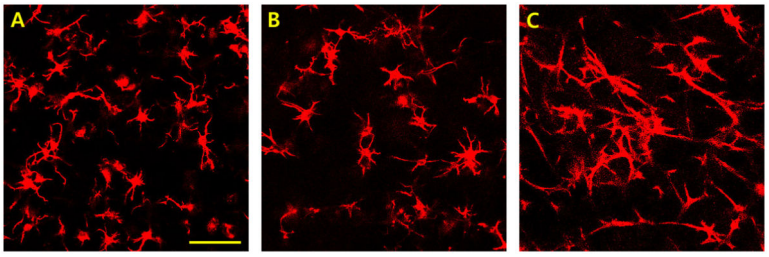

Figure 9.

Confocal microscopy images of actin-stained human dermal fibroblasts encapsulated within 6% w/v blended PEGdA (C1-12.5% PEG-bis-AA, 37.5% PEG-bis-AP, 50.0% PEG-bis-AB)/0.36% HA semi-IPNs at 200 μm depth after 7 days (A), 21 days (B), and 35 days (C) culture, scale bar = 100 μm.

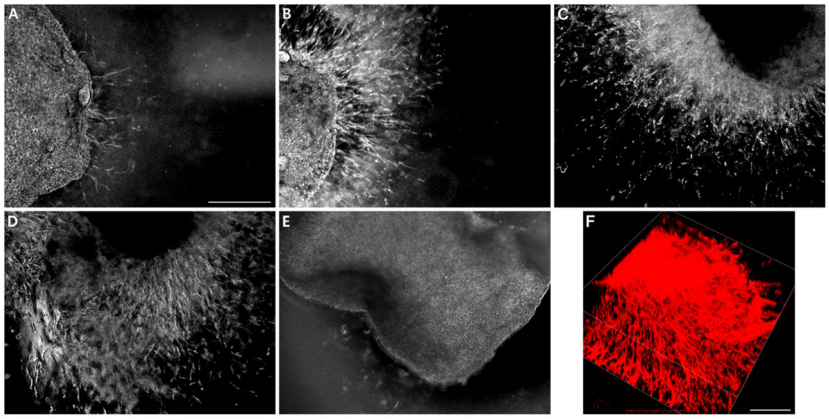

Figure 10.

Migration of human dermal fibroblasts pre-encapsulated within 1% w/v fibrin clots into surrounding 6% w/v blended PEGdA (C1-12.5% PEG-bis-AA, 37.5% PEG-bis-AP, 50.0% PEG-bis-AB)/0.36% w/v HA semi-IPNs after 3 days (A), 7 days (B), 14 days (C) 21 days (D) and 6% w/v blended PEGdA (C1)/0.36% w/v GMHA copolymer hydrogels after 21 days (E) culture. 3D confocal reconstruction of fibroblasts migrating from fibrin clots into surrounding 6% w/v blended PEGdA (C1)/0.36% w/v HA semi-IPN after 14 days in culture (F). Scale bars = 500 μm.

Table 1

Semi-IPN hydrogel compositions.

Variable	[HA]*	HA MW (MDa)	PEGdA chem.	[PEGdA]*
[HA]*	0 – 0.72	1.5	PEG-bis-AP	6
HA MW	0.36	0.1 – 1.5	PEG-bis-AP	6
PEGdA chem.	0.36	1.5	PEG-bis-AA, AP, AB	6
[PEGdA]*	0.24 – 0.6†	1.5	PEG-bis-AP	4.0 – 10.0

*All concentrations were based on % w/v

†HA concentration was varied to keep the ratio between PEGdA and HA constant at 6% w/v